ELSEVIER

Journal of Molecular Catalysis A: Chemical 188 (2002) 133–139

JOURNAL OF MOLECULAR CATALYSIS A: CHEMICAL

www.elsevier.com/locate/molcata

Liquid phase acetophenone hydrogenation on Ru/Cr/B catalysts supported on silica

Manuela Casagrande [a], Loretta Storaro [a], Aldo Talon [a], Maurizio Lenarda [a,*], Romana Frattini [b], Enrique Rodríguez-Castellón [c], Pedro Maireles-Torres [c]

[a] *Dipartimento di Chimica, Università di Venezia Ca' Foscari, Via Torino 155B, and INSTM-UdR di Venezia, 30100 Mestre-Venezia, Italy*
[b] *INFM and Dipartimento di Chimica Fisica, Università di Venezia Ca' Foscari, Via Torino 155B, 30100 Mestre-Venezia, Italy*
[c] *Departamento de Quìmica Inorgánica, Cristalografia y Mineralogía, Universidad de Málaga, Apdo. 59, 29071 Málaga, Spain*

Received 12 December 2001; received in revised form 19 February 2002; accepted 19 February 2002

Abstract

The liquid phase hydrogenation of acetophenone was studied over a series of silica supported bimetallic catalysts with various Ru/Cr atomic ratios. The catalysts were prepared by reduction of the metal salts with $NaBH_4$ aqueous solutions and were characterised by X-ray diffraction (XRD) and X-ray photoelectron spectroscopy (XPS) (ESCA). The hydrogenation reaction was carried out in batch at a hydrogen pressure of 9 bar. The selectivity towards reduction of the carbonyl function increases with the increasing amount of Cr ions added.

Keywords: Hydrogenation; Acetophenone; Ruthenium/chromium catalysts; Catalysts characterisation; XPS; XRD

1. Introduction

The catalytic hydrogenation of organic derivatives containing a carbonyl group, is a reaction widely used in the preparation of intermediates for the fine chemicals and pharmaceutical industries. The hydrogenation of acetophenone is particularly important because of the extensive industrial use of two of the possible reaction products: 1-phenyl ethanol (PE) and 1-cyclohexyl ethanol (CHE). In fact, CHE is employed in the manufacturing of some polymers, while PE finds use in the pharmaceutical and perfume industries. The reaction is usually carried out in the liquid phase, at low hydrogen pressure, using transition metals supported on zeolites or oxides as catalysts [1–6]. Bimetallic systems [7–9] are often preferred in order to obtain better activity, stability and selectivity of the catalytic systems.

Ruthenium, on various oxidic supports, has been used for the selective catalytic hydrogenation of aromatics and carbonyl groups [10,11]. Bimetallic ruthenium/tin based systems, in particular, were successfully used in the hydrogenation of carbonylic and carboxylic derivatives [12–16]. Chromium ions have been used as promoters in Raney nickel based catalysts for the selective acetophenone reduction [7–9]. In this paper, we present the results of a study on the liquid phase hydrogenation of acetophenone using silica supported ruthenium based catalysts, promoted by chromium ions, which are prepared by reduction at room temperature with aqueous sodium tetrahydroborate.

* Corresponding author. Tel.:+39-0412346762; fax: +39-0412346735.
E-mail address: lenarda@unive.it (M. Lenarda).

1381-1169/02/$ – see front matter
PII: S1381-1169(02)00079-1

2. Experimental

2.1. Materials

Acetophenone, PE, cyclohexyl methyl ketone (CHMK), *n*-hexane, $NaBH_4$, $RuCl_3{\cdot}3H_2O$ and $CrCl_3{\cdot}6H_2O$ were Aldrich Chimica products, while hydrogen was from SIAD.

Silica was a 432(7)Grace silica catalyst support, with a surface area of 320 m^2/g and pore volume of 1.65 ml/g.

2.2. Catalysts preparation

The loading of ruthenium was fixed to 2% (w/w). A series of catalysts, with Ru/Cr molar ratios 4:1, 1:1, and 1:4, respectively, and identified as RuCrB/SIL(4/1), RuCrB/SIL(1/1), and RuCrB/SIL(1/4), respectively, were prepared as described below.

An aqueous solution of $RuCl_3{\cdot}3H_2O$ and $CrCl_3{\cdot}6H_2O$ was added to a vigorously stirred aqueous slurry of SiO_2. The resulting mixture was left to stand for 2 h.

Then an aqueous solution of sodium borohydride (molar ratio Ru:$NaBH_4$, 1:400) was added dropwise to the slurry. After the reduction was completed, the catalyst was filtered, washed first with distilled water and successively with acetone and then vacuum dried for 3 h.

The sample RuB/SIL was prepared by SiO_2 impregnation with an aqueous solution of $RuCl_3{\cdot}3H_2O$. The suspension was left to stand for 2 h. The reduction with $NaBH_4$ was carried out as described above for the other samples.

2.3. Powder X-ray diffraction (XRD)

The X-ray diffraction patterns were collected with a Bragg–Brentano powder diffractometer using Cu Kλ radiation ($\lambda = 1.5418$ Å) and a monochromator in the diffracted beam. Diffraction data were analysed with the Rietveld method [17], using the RIETQUAN codes [18]. This program, in a fully automated version, is particularly suited for a quantitative evaluation of the phases present in the X-ray diffraction patterns. The parameters of physical meaning, such as lattice constant, phase abundance, average crystallite size and microstrain, are worked out from the full pattern analysis and not by comparative investigation of the peak broadening after analysis for each peak [19].

2.4. X-ray photoelectron spectroscopy (XPS) (ESCA)

X-ray photoelectron spectra were obtained using a Physical Electronics PHI 5700 spectrometer with a non-monochromatic Mg Kα radiation (300 W, 15 kV, 1253.6 eV) as excitation source. High-resolution spectra were recorded at a 45° take-off-angle by a concentric hemispherical energy electron analyser, operating in the constant pass energy mode at 29.35 eV, using a 720 μm diameter analysis area. Under these conditions, the Au $4f_{7/2}$ line was recorded with 1.16 eV FWHM at a binding energy of 84.0 eV. The spectrometer energy scale was calibrated using Cu $2p_{3/2}$, Ag $3d_{5/2}$ and Au $4f_{7/2}$ photoelectron lines at 932.7, 368.3, and 84.0 eV, respectively. Charge referencing was done against Si 2p at 103.1 eV, because the signal C 1s is overlapped with the Ru $3d_{3/2}$ peak. Samples were mounted on a sample holder without adhesive tape and kept overnight at high vacuum in the preparation chamber, before they were transferred to the analysis chamber of the spectrometer for the measure. Each spectral region was scanned with several sweeps till a good signal to noise ratio was observed. Survey spectra in the range 0–1200 eV were recorded at 187.85 eV of pass energy. The pressure in the analysis chamber was maintained lower than 5×10^{-6} Pa. The PHI ACCESS ESCA-V6.0 F software package was used for acquisition and analysis of the data. A Shirley-type background was subtracted from the signals. Gauss–Lorentz curves (maximum 20% Lorentz) were used for the fitting of the recorded data. Atomic concentration percentages of samples were determined taking into account the corresponding area sensitivity factor for the different measured spectral regions. The absolute errors in atomic concentration are 1.0% for carbon, 2.0% for oxygen, 2.0% for Si, and ca. 5% for the other elements. For scaling reasons, the intensity of each spectrum was normalised at its maximum value in all the XPS figures.

2.5. Catalytic acetophenone hydrogenation

The reactions were carried out in a 230 ml stainless steel autoclave. In a typical hydrogenation experiment,

100 mg of catalyst, 10 ml of solvent and 4.3 mmol of acetophenone were charged into the autoclave.

The reactor was purged with hydrogen four times, to remove the air, then was pressurised up to 9 bar and heated to 333 K. The reacting mixture was stirred at 500 rpm. After the required reaction time, the reactor was cooled to room temperature and the reaction mixture recovered for analysis. The products were analysed by gas chromatography (Hewlett Packard 6890) with a HP-5 capillary column and with a FID detector.

3. Results and discussion

3.1. Catalysts characterisation

3.1.1. XRD measurements

All the samples were analysed by powder XRD. Experimental profiles were fitted according to the Rietveld methods, and the results are shown in Fig. 1. In Table 1, the obtained phase abundance, average crystallite size, lattice strain values are reported.

All the samples were found to have a phase fraction value corresponding to a Ru content (% w/w), that corresponds to one half the theoretical loading, planned for the catalyst. This finding was confirmed by the Atomic Adsorption data. The metal particles resulted all of nanometric dimensions, with $\langle D \rangle$ values inferior to 2 nm. Crystalline phases of chromium oxides were not found. Nevertheless, the presence of Cr and B species appear to cause a modification of the lattice parameters, that resulted, respectively, in values of $a = b = 2.9674$ and $c = 4.7304$ versus the values of $a = b = 2.7058$ and $c = 4.282$ reported in the literature [20].

Table 1
Structural parameters of the reported samples, obtained with the Rietveld fit

Sample	Phase fraction Ru/Si (% w/w)	Particles dimension $\langle D \rangle$ (nm)	Average mean square strain $\langle \varepsilon^2 \rangle^{1/2}$
RuB/SIL	1.2	2	$2e^{-2}$
RuCrB/SIL(4/1)	0.9	1	$3e^{-2}$
RuCrB/SIL(1/1)	1.0	1	$3e^{-2}$
RuCrB/SIL(1/4)	0.5	$\cong 1$[a]	$1e^{-2}$

[a] The peak is too weak and broad to allow a clear evaluation of the phase fraction and particles dimension.

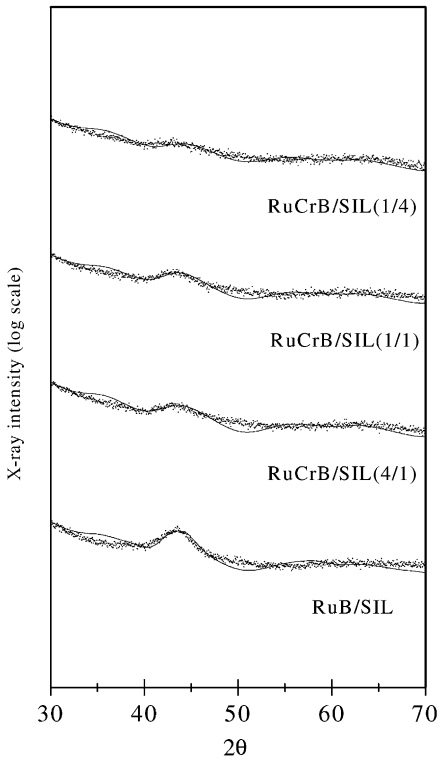

Fig. 1. X-ray diffraction patterns (logarithmic scale) vs. 2θ of the indicated specimens. Data points refer to experimental data and full lines to a fit according to the Rietveld methods. The broad peak at $2\theta \cong 43^\circ$ refers to a Ru nanocrystalline phase. The satisfactory goodness of the fit (R_{wp} values between 5 and 7%) enable us to determine the final structural parameters in terms of physically meaningful quantities, i.e. phase abundance, average crystallite size, and lattice strain.

3.1.2. ESCA measurements

All the bimetallic catalysts samples were analysed by ESCA and binding energies (eV) and XPS ratios Ru/Cr^{n+} are reported in Table 2.

A survey of the XPS spectra showed evidence of the presence of C 1s, O 1s, Si 2p, Ru 3d, and Cr 2p in the chromium containing samples, and in the remaining sample also, evidence of B 1s along with Na 1s, Si 2p and O 1s correspond to SiO_2.

3.1.2.1. RuB/SIL. The Ru $3d_{3/2}$ peak overlaps with the C 1s signal, but the Ru $3d_{5/2}$ can be seen without problems. The position of Ru $3d_{5/2}$ peak at 280.0 eV corresponds to Ru(0), while the peak at 282.0 eV to Ru(III), with a corresponding Ru(0)/Ru(III) ratio of

Table 2
Binding energies (eV) and XPS atomic ratios for reported samples

Sample	Ru $3d_{5/2}$	Cr $2p_{3/2}$	Ru/Cr^{n+}
RuB/SIL	280.0 ± 0.5	–	–
	282.0 ± 0.5		
RuCrB/SIL(4/1)	279.0 ± 0.5	576.0 ± 0.5	1.2
	281.0 ± 0.5		
RuCrB/SIL(1/1)	280.0 ± 0.5	577.0 ± 0.5	0.22
	282.0 ± 0.5		
RuCrB/SIL(1/4)	280.0 ± 0.5	577.0 ± 0.5	0.05
	282.0 ± 0.5		

3/1. The presence of still unreduced ruthenium species can be explained by the fact that the samples have been handled in air.

B 1s has a very noisy signal with a maximum at 193.0 ± 0.5 eV corresponding to an oxidised boron species.

3.1.2.2. RuCrB/SIL(4/1). The Ru $3d_{5/2}$ signal is asymmetric and the doublet Ru $3d_{3/2}$ overlaps the C 1s signal. Anyway, the Ru $3d_{5/2}$ signal was analysed and can be described as the combination of a peak corresponding to Ru(0) 65% at 279.0 ± 0.5 eV and one to Ru(III) 35% at 281.0 ± 0.5 eV. The Cr $2p_{3/2}$ signal indicates the existence of Cr(III) 77% at 576.0 ± 0.5 eV and Cr(VI) 23% at 579.0 ± 0.5 eV.

3.1.2.3. RuCrB/SIL(1/1). The Ru $3d_{3/2}$ peak overlaps the C 1s signal, but the Ru $3d_{5/2}$ can be seen without problems. The broad peak at 281.0 eV can be decomposed in two peaks at 280.0 and 282.0 eV, corresponding to Ru(0) 52% and Ru(III) 48% (Fig. 2).

B 1s is very noisy with two maxima at 192.0 ± 0.5 and 193.0 ± 0.5 eV, clearly due to boron being in an oxidised state. The Cr $2p_{3/2}$ peak was found at 577.0 ± 0.5 eV, and corresponds to the presence of only Cr(III); no Cr(VI) was detected.

3.1.2.4. RuCrB/SIL(1/4). The Ru $3d_{5/2}$ signal was deconvoluted in two contributions, one at 280.0 ± 0.5 eV that corresponds to Ru(0) 61%, and the other at 282.0 ± 0.5 eV, corresponding to Ru(III) 39%.

The B 1s signal is very noisy with a maximum at 193.0 ± 0.5 eV. Cr $2p_{3/2}$ peak is at 577.0 ± 0.5 eV and corresponds to the presence of Cr(III); no Cr(VI) was detected.

It can be easily seen from the ESCA data, that the Ru/Cr species ratios (1.2, 0.22, and 0.05) observed on

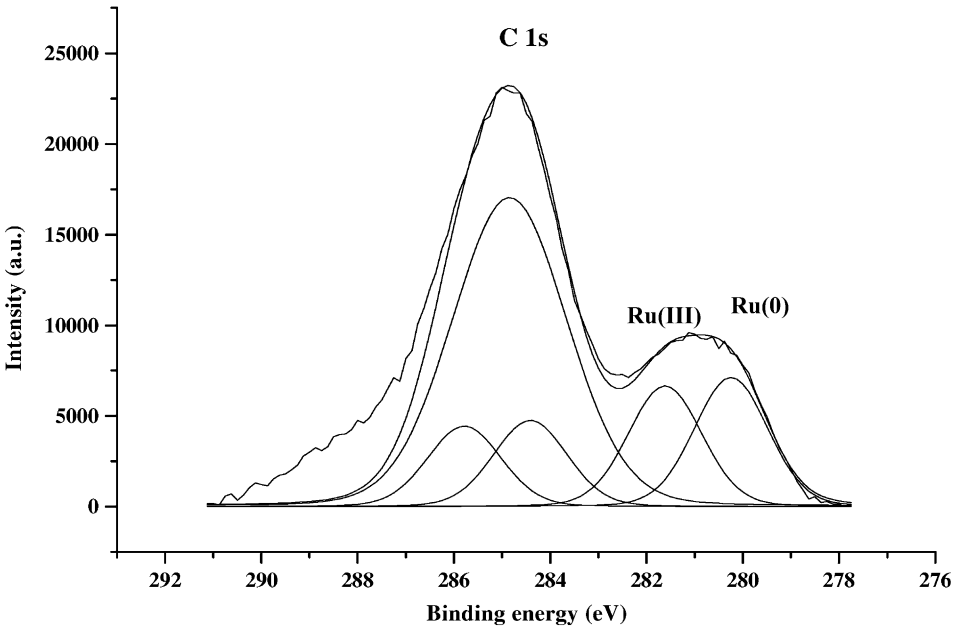

Fig. 2. XPS spectrum of RuCrB/SIL(1/1).

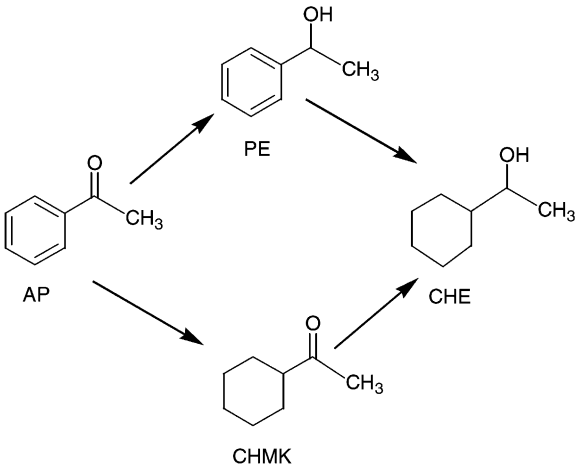

Scheme 1. Reaction scheme for the hydrogenation of acetophenone. AP: acetophenone; PE: 1-phenyl ethanol; CHMK: cyclohexyl methyl ketone; CHE: 1-cyclohexyl ethanol.

the catalyst surface are quite different from the Ru/Cr ions ratios (4, 1, and 0.25) of the solution used in the catalysts' preparation, resulting in effective Ru/Cr ratios approximately one fourth of the theoretical. This finding clearly can be an indication of a partial coverage of the ruthenium nanoparticles by oxidised Cr species.

3.2. Catalytic tests

The acetophenone hydrogenation has a quite complex reaction scheme (Scheme 1) that has been the subject of several mechanistic studies [3–5]. The reduction, in fact, of the carbon–oxygen double bond gives PE, the hydrogenation of the aromatic ring gives the CHMK, and both compounds undergo further hydrogenation to CHE.

Table 3
Product distribution and total conversion after 1 h reaction time for the studied catalysts

Catalyst	Ru/Cr (ESCA)	Conversion (%)	Product (%)		
			PE	CHMK	CHE
RuB/SIL	–	90	22	36	42
RuCrB/SIL(4/1)	1.2	59	58	22	20
RuCrB/SIL(1/1)	0.22	33	67	21	12
RuCrB/SIL(1/4)	0.05	26	70	20	10

Conversion (%): moles of acetophenone reacted/moles of acetophenone introduced per cent.

Product distribution data for all studied catalysts after 1 h of reaction time are reported in Table 3 and Fig. 3.

The monometallic RuB/SIL catalyst showed quite a high catalytic activity with 90% conversion after 1 h of reaction. Nevertheless, the catalyst is not selective, the reaction mixture being in fact constituted after 1 h of reaction by a mixture of the aromatic alcohol (PE) and the alicyclic ketone (CHMK) formed by hydrogenation of the aromatic ring, and by the totally reduced alicyclic alcohol (CHE) that can be generated both by the reduction of PE and CHMK. The aromatic ring hydrogenation appeared to be the prevailing reaction. This is not surprising due to the nanometric dimensions of the metal particles and the well-known hydrogenation ability of ruthenium catalysts [10,21]. After 90 min, all the acetophenone is converted and after 3 h the only product detected was alicyclic alcohol (CHE).

When chromium ions were added to the ruthenium catalyst until an effective Ru/Cr atomic ratio of 1.2

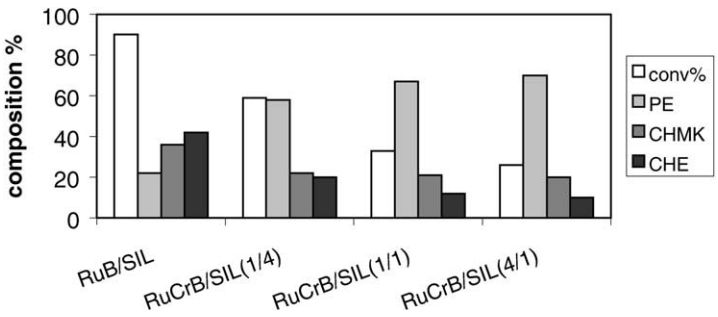

Fig. 3. Product distribution and total conversion after 1 h of reaction time for the studied catalysts.

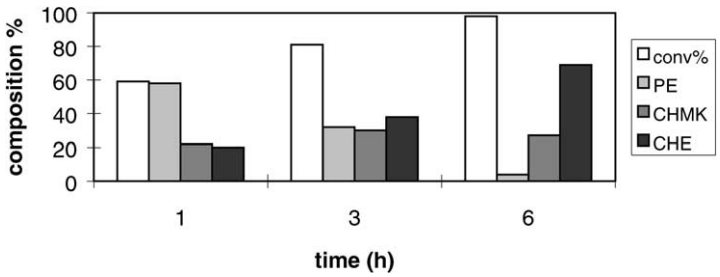

Fig. 4. Products distribution and conversion versus reaction time over RuCrB/SIL(4/1) catalyst.

was reached on the surface, the selectivity towards the reduction of the carbonyl function sharply increased. In fact, after 1 h of reaction (Table 3, Fig. 3), the PE production increased by 36%, while that of CHMK decreased by 14%, and the overall acetophenone conversion decreased by 30%. Addition of more Cr ions (Ru/Cr = 0.22) caused a further 30% decrease of the conversion, but only an 11% increase of the PE production. A further decrease of the Ru/Cr atomic ratio to 0.05 resulted only in slight modifications of the product distribution.

In Fig. 4, a typical course of acetophenone transformation on the Ru/Cr catalyst RuCrB/SIL(4/1) is reported as an example.

In Table 4, the product distribution data at various reaction times for the same catalyst are summarised.

The enhanced selectivity of the mixed metals catalytic systems toward the hydrogenation of the acetophenone carbonyl function can be attributed to the creation of new active sites of the type $M–M_1^{3+}$. On these sites, the carbonyl group is activated by the bonding of the oxygen atom to the oxophylic Cr^{3+}cations that facilitates the attack of the hydride on the catalyst surface [7–9]. Addition of increasing amounts of chromium ions causes an initial strong selectivity rise toward the carbonyl reduction but successive additions only slightly modify the product distribution. A decrease of the conversion was observed as chromium ions are added to the ruthenium catalysts. ESCA measurements showed that the Ru^0/Ru^{3+}ratio on the catalyst surface decreases as the Cr content increases. Nevertheless, the Ru^0/Ru^{3+} ratio is observed to go from 3/1 to 2/1 and 1/1, as the Ru/Cr ratio decreased from pure Ru to Ru/Cr (4/1) and Ru/Cr (1/1). Further chromium additions (Ru/Cr, 1/4) left the Ru^0/Ru^{3+} ratio almost unaltered. These findings can be explained, supposing that the increasing amounts of chromium ions added probably prevented the complete reduction of the ruthenium cations during the catalysts' activation, resulting in a strong decrease of the hydrogenation activity. On the other hand, a mere physical coverage of the ruthenium active sites by Cr oxidised species evidenced by ESCA data, surely contributes to the activity reduction. It is consequently readily explainable that, while the initial addition of Cr ions to the starting solution used to obtain RuCrB/SIL(4/1) strongly increased the selectivity, but only slightly affected the overall activity, the further addition of Cr caused a slight selectivity increase, coupled to a strong activity decrease, and in spite of the overwhelming amount of Cr ions added (Ru/Cr = 0.05), the RuCrB/SIL(1/1) and RuCrB/SIL(1/4) gave similar performances.

Table 4
Product distribution and total conversion for increasing reaction times for the RuCrB/SIL(4/1) catalyst

Reaction time (h)	Conversion (%)	Product (%)		
		PE	CHMK	CHE
1	59	58	22	20
3	81	32	30	38
6	98	4	27	69

Conversion (%): moles of acetophenone reacted/moles of acetophenone introduced per cent.

4. Conclusions

We can conclude that, room temperature reduction of a solution of ruthenium salt with aqueous sodium borohydride slurried with silica allows the preparation

of nanostructured catalysts that resulted very active in the low-pressure hydrogenation of acetophenone. The addition of chromium salts to the starting solution gave rise to catalysts, with an increased selectivity toward the reduction of the carbonyl function, but at the same time depressed the overall catalyst performance. The selectivity increase is attributable to the strong interaction of the oxygen atom of the carbonyl with the Cr ions. The overall hydrogenation activity decrease can be due both to the minor reducibility of the Ru ions caused by the presence of adjacent chromium ions, and to the partial coverage of the reduced ruthenium surface active sites by aggregates of chromium(III) oxide.

Acknowledgements

This work was supported by funds of the Ministero dell'Università e Ricerca Scientifica MURST (Fondo d'Ateneo) and by the Italian National Research Council (CNR, Rome (I)—Programma "Chimica" L.95/95).

References

[1] M.A. Aramendia, V. Borau, C. Jiménez, J.M. Marinas, M.E. Sempere, P. Urbano, Appl. Catal. 43 (1988) 41.
[2] P.S. Kumbhar, Appl. Catal. A: Gen. 96 (1993) 241.
[3] I. Bergault, P. Fouilloux, C. Joly-Vuillemin, H. Delmas, J. Catal. 175 (1998) 328.
[4] N. Lavaud, P. Magnoux, F. Alvarez, L. Melo, G. Giannetto, M. Guisnet, J. Mol. Catal. A Chem. 142 (1999) 223.
[5] M.V. Rajashekharam, I. Bergault, P. Foilloux, D. Schweich, H. Delmas, R.V. Chaudhari, Catal. Today 48 (1999) 83.
[6] I. Bergault, C. Joly-Vuillemin, P. Fouilloux, H. Delmas, Catal. Today 48 (1999) 161.
[7] S. Hamar-Thibault, J. Masson, P. Fouilloux, J. Court, Appl. Catal. A: Gen. 99 (1993) 131.
[8] J. Masson, S. Vidal, P. Cividino, P. Fouilloux, J. Court, Appl. Catal. A: Gen. 99 (1993) 147.
[9] R.V. Malyala, C.V. Rode, M. Arai, S.G. Hedge, R.V. Chaudhari, Appl. Catal. A: Gen. 193 (2000) 71.
[10] P. Kluson, L. Cerveny, Appl. Catal. A: Gen. 128 (1995) 13.
[11] P. Kluson, L. Cerveny, J. Mol. Catal. A 108 (1996) 107.
[12] M. Toba, S. Tanaka, S. Niwa, F. Mizukami, Z. Koppàny, L. Guczi, K.-Y. Cheah, T.-S. Tang, Appl. Catal. A: Gen. 189 (1999) 243.
[13] C.S. Narasimhan, V.M. Deshpande, K. Ramnarayan, Indian Eng. Chem. Res. 28 (1989) 1112.
[14] V.M. Deshpande, W.R. Patterson, C.S. Narasimhan, J. Catal. 121 (1990) 165.
[15] V.M. Deshpande, K. Ramnarayan, C.S. Narasimhan, J. Catal. 121 (1990) 174.
[16] B. Coq, P.S. Kumbhar, C. Moreau, P. Moreau, F. Figueras, A. Young, J. Phys. Chem. 98 (1994) 10180.
[17] The Rietveld Method, R. International Union of Crystallography, Oxford University Press, Oxford, 1993.
[18] L. Lutterotti, S. Gialanella, Acta Mater. 46 (1998) 101.
[19] M. Lenarda, R. Ganzerla, L. Storaro, R. Frattini, S. Enzo, R. Zanoni, J. Mater. Res. 11 (1996) 325.
[20] National Bureau of Standards, Circular 539, Vol. IV, 1955, p. 5.
[21] G.A. Olah, A. Molnàr, Hydrocarbon Chemistry, Wiley, New York, 1995.